Journal of Environment and Earth Science
ISSN 2224-3216 (Paper) ISSN 2225-0948 (Online)
Vol. 3, No.11, 2013

Analysis and Interpretation of In-Phase Component of VLF-EM Data using Hilbert Transform and the Amplitude of Analytical Signal

Lazarus G. Ndatuwong[1,2*] and G. S. Yadav[1]
1.Banaras Hindu University, Department of Geophysics, 221005 – Varanasi, India.
2.Adamawa State University, Department of Physics, PMB 25-Mubi, Adamawa State–Nigeria
*E-mail of the corresponding author: ndatuwong@gmail.com.

Abstract
An interpretation of in-phase anomaly of very low frequency electromagnetic (VLF-EM) data was carried out using the analysis of the Hilbert transform of the in-phase component and the amplitude of its analytic signal. The analysis was used to delineate the source and depth to the top of a subsurface conductive body. The amplitude of the analytical signal of the data was observed to mimic the conventional Fraser-filtered operation and was used to locate the exact location of the anomalous body. The in-phase component with the Hilbert transform yields an approximate depth to the top of the conductor which agree with the result of the vertical electrical sounding conducted at the vicinity of the anomalous body.
Keywords: VLF-EM method, Hilbert transform, analytical signal, in-phase, Fraser filtering.

1. Introduction

The anomaly observed in any geophysical survey is usually associated with the deviation of the measured signal from the normal level, and this deviation is a result of the response of the subsurface geological objects of interest. The measured signal can be processed for locating the geological structures which are causing the anomaly and then quantitatively interpreted in terms of depths, width, dip, physical properties etc. There are many well-known methods for processing and interpretation of geophysical signals particularly employing integral transforms like Fourier, Hilbert, Mellin, Hartley (Nabighian 1972; Mohan *et al*. 1982; Mohan *et al*. 1986; Sundararajan & Ramabrahmam 1997; Sundararajan *et al*. 1998).

In VLF-EM geophysical survey, both the in-phase and quadrature components of VLF-EM data contain valuable diagnostic information about the subsurface targets. However, only a few schemes exist for extracting the required information and thereby relating the observed anomalies to the causative source. Although the conventional Fraser and Karous–Hjelt filtering techniques provide first hand information regarding the relative disposition of the discrete conductors, the disadvantage with these filters is that it causes a loss of 20 to 30% of data on either side of the profile, which sometimes complicates the interpretation of the data (Sundararajan *et. al*. 2011). In this study the interpretation procedures employ the use of amplitude analysis of in-phase component of VLF-EM data and its Hilbert transform to provide information about the depth to the top of the conducting body. The interpretation is based mainly on certain characteristic points of the amplitude of the analytical signal and the abscissa of the point of intersection of the in-phase component and its Hilbert transform.

2. Study area

Geologically the study area is part of the Kaimur series of the Upper Vindhyan Supergroup located in the southern part of Uttar Pradesh State (Figure 1). The area falls within the survey of India toposheets 63L/9, 63L/10, 63L/13, 63L/14. The Vindhyan Supergroup is composed mostly of low dipping formations of sandstone, shale and carbonate, with a few conglomerate and volcaniclastic beds, separated by a major regional and several local unconformities (Bhattacharyya 1996). The regional unconformity occurs at the base of the Kaimur Group and divides the sequence into two units: the Lower Vindhyans (Semri Group) and the Upper Vindhyans (Kaimur, Rewa and Bhander Groups). The outcrop pattern of the Supergroup resembles a simple saucershaped syncline. It is generally believed that the Vindhyan basin was a vast intra-cratonic basin formed in response to intraplate stresses (Bose *et al*. 2001). The Kaimur consists of a lower shale unit overlain by quartz rich sandstone containing basin wide volcaniclastic deposit. Sandstones and quartzites are prominent horizons with wide distribution in the Kaimur Group. All the major sandstone horizons form the scrap while the shale horizons form gentle slopes (Bose *et al*. 2001).

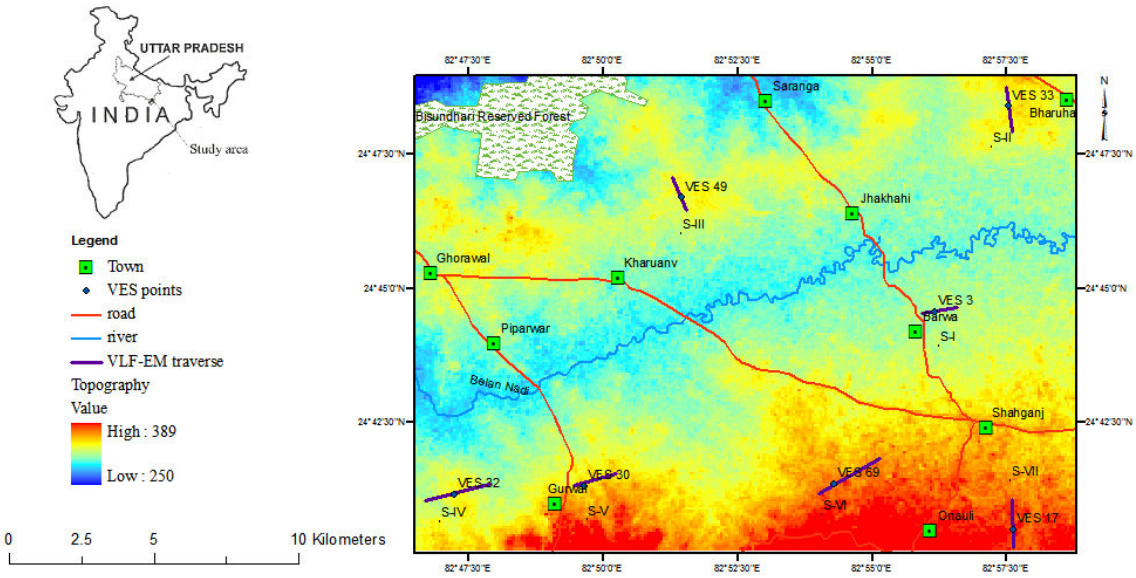

Figure 1. Site map and VLF-EM traverse location.

3. Basic theory of vlf-em method

The very low frequency – electromagnetic (VLF-EM) technique is a passive method that uses radiation from ground-based military radio transmitters as the primary EM field for geophysical survey. These transmitters generate plane EM waves that can induce secondary eddy currents, particularly in electrically conductive elongated 2-D targets. The EM waves propagate through the subsurface and are subjected to local distortions by the conductivity contracts in this medium. These distortions indicate the variations in geoelectrical properties which may be related to the presence of groundwater (Shendi 1997). The subsurface occurrence of these conductive bodies creates a local secondary field which has its own components. Measurement of these components may be use as an indicator for locating the subsurface conductive zones.

The VLF-EM waves travel in three modes: skywave, spacewave (wave-guided by the ionosphere and earth surface), and groundwave. As the groundwave is attenuated through long distances, only the skywave and spacewave are received as the primary wave (Jeng *et al*. 2004). The depth of penetrations of these waves depends on the frequencies and the electrical conductivity of the ground. This depth increases as both the frequencies and ground conductivity decreases as (keary and Brooks 1984)

$$\delta = \sqrt{\frac{2}{\mu_o \sigma w}} \cong \frac{500}{\sqrt{\sigma f}} = 500\sqrt{\frac{\rho}{f}} \quad (1)$$

where;

δ = Skin depth in meters (i.e the depth of penetration of a wave passing into a conductor in which the amplitude of the wave is attenuated to 1/e of its amplitude at the surface of the conductor).

μo = Magnetic permeability of free space $= 4\pi \times 10^{-7}$ Henry/m.

w = Angular frequency (2πf)

σ = Electrical conductivity of earth material (mho/m) (Inverse of resistivity, ρ)

f = Signal frequency.

At very large distances from a source of electromagnetic waves, attenuation of this type would control the depth of exploration. Effective depth of exploration, Ze, defines the maximum depth a body can be buried and still produce a signal recognizable above the noise. It is given as (keary and Brooks 1984)

$$Z_e = 100\sqrt{\frac{\rho}{f}} \quad (2)$$

For VLF-EM, the frequencies are too high for much penetration, so that the method is useful only for shallow geologic mapping. According to Fischer et al. (1983), VLF ground surveys provide a quick and powerful tool for the study of geologic features within about 100 m of the surface.

The magnetic component of the VLF wave is mainly used for field measurement. According to the basic EM theory, the primary EM field is shifted in phase when encountering a conductive body and the conductive body then becomes the source of a secondary field. The VLF instrument detects the primary and secondary fields, and separates the secondary field into in-phase and quadrature components based on the phase lag of the secondary field. These two components of the secondary field are sometimes referred to as the tilt (in-phase) and ellipticity (quadrature). When the VLF-EM method is used for geophysical survey, the in-phase response is sensitive to

metal or good conductive bodies. The quadrature response, on the other hand, is sensitive to the variation of the earth electrical properties (Jeng *et al*. 2004).

4. Material and method

VLF-EM data were collected using WADI instrument manufactured by ABEM. For the purpose of this work, seven traverses were conducted at seven different locations where electrical sounding were conducted. The equipment used measured the real (in phase) and quadrature (out of phase) components of the vertical to horizontal magnetic field ratio.

The electrical soundings were conducted using ABEM SAS 1000 Terrameter.

4.1. Hilbert transform

The use of Hilbert transform for interpretation of VLF-EM data for possible depth estimation is analogy with the interpretation of gravity/magnetic/self potential data data (Sinha 1990; Sundararajan & Srinivas 1996; Ramesh Babu *et. al*. 2007). Hilbert transform is a phase shifter of 90 degrees or a linear operation which corresponds to a filter by means of which the amplitude of the spectral components remain unchanged but the phase is advanced by 90 degrees for positive frequencies and retarded by 90 degrees for negative frequencies (Thomas 1969). It is mathematically expressed as

$$H(x) = \frac{1}{\pi}\int_0^{\infty}[IF(\omega)\cos(\omega x) - RF(\omega)\sin(\omega x)]d\omega \quad (3)$$

where RF(w) and IF(w) are the real and imaginary parts of the Fourier transform of f(x) expressed as

$$F(w) = \int_{\infty}^{-\infty} f(x)\mathrm{e}^{-\omega \mathrm{x}\mathrm{t}}dx = RF(\omega) - iIF(\omega) \quad (4)$$

4.2. Amplitude of analytical signal

The amplitude of the analytical signal is a key factor that is extensively used for locating the precise origin of subsurface features beside its role in estimating the depth to the top of the feature in the interpretation of gravity, magnetic and self-potential anomalies. The amplitude of the analytical signal gives a symmetrical curve and in general attains its maximum exactly over the origin of regular geometrical structures; however, the peak of the amplitude corresponds to the origin for all structures (Sundararajan *et. al*. 2011). This property exhibited by the amplitude of analytical signal is highly useful to determine the exact spatial location of sources. For VLF-EM anomaly, if f(x) is the in-phase component and H(x) its Hilbert transform, then the analytical signal can be expressed as

$$A(x) = f(x) - iH(x) \quad (5)$$

and the amplitude of the analytical signal as

$$AA(x) = \sqrt{f(x)^2 + H(x)^2} \quad (6)$$

Based on certain characteristic points of the amplitude of the analytical signal and the abscissa of intersection of the in-phase components and its Hilbert transform, the dept to the top of a targeted anomaly can be estimated. Work done on potential fields of magnetic and SP anomaly shows that the dept to the top of a detected anomaly is the abscissa of the point of intersection of the anomaly and the Hilbert transform (Sundararajan *et. al*. 1985; Sundararajan & Srinivas 1996). In this study, we used the intersection points x_1 and x_2 from the in-phase component and its Hilbert transform with certain characteristic points of the amplitude of the analytical signal to determine the depth to top of the conductor. The depth, h, can be estimated as (Dondurur & Pamukcu 2003, Sundararajan & Srinivas 2010)

$$h = \frac{x_1 + x_2}{2} \quad (7)$$

5. Result and discussion

A plot of the in-phase, quadrature, Fraser-filtered and amplitude analytical signal of the in-phase component of seven traverses, located in seven different locations as seen in Figure 1 was first carried out in order to compare how well the Fraser-filtered and the amplitude analytical signal can be used to locate the exact position of an anomaly. The result for all the traverses Figure 2(a) shows how the maximum of the bell-shape symmetrical curve of the amplitude analytical signal compares very well with the peak of the Fraser-filtered data over the crossover points between the in-phase and quadrature (indicated with an arrow). A qualitative interpretation of VLF-EM data is based on the cross-over point between the real and imaginary data which appears as positive peaks in the Fraser-filtered real curve, these regions constitute anomalous zones which can be attributed to the presence of vertical conductor or lateral contacts of different resistivities beneath the surface (Srigutomo *et al*. 2005). This therefore ascertains a simple fact that the amplitude analytical signal of the in-phase component mimics the Fraser-filtered of the in-phase component as seen in Figure 2(a).

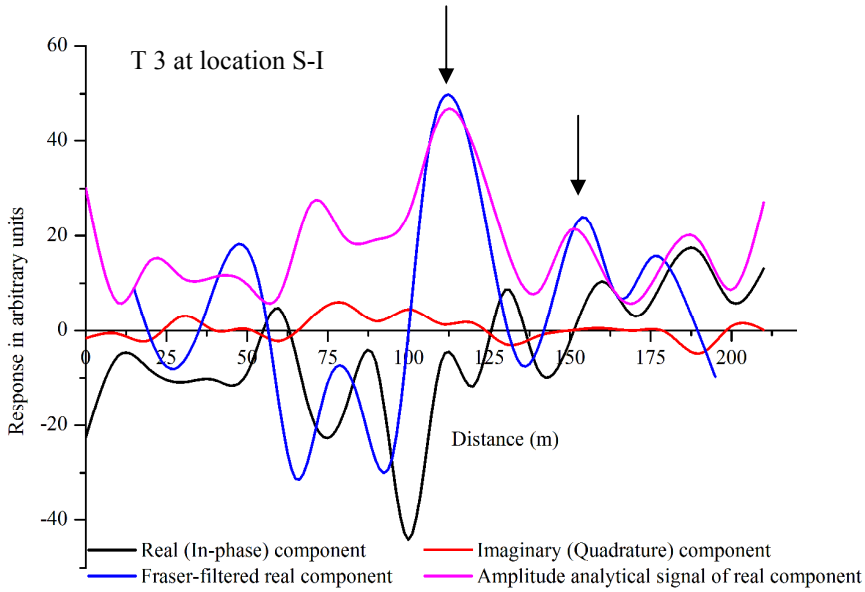
T 3 at location S-I
Response in arbitrary units
Distance (m)
Real (In-phase) component
Imaginary (Quadrature) component
Fraser-filtered real component
Amplitude analytical signal of real component

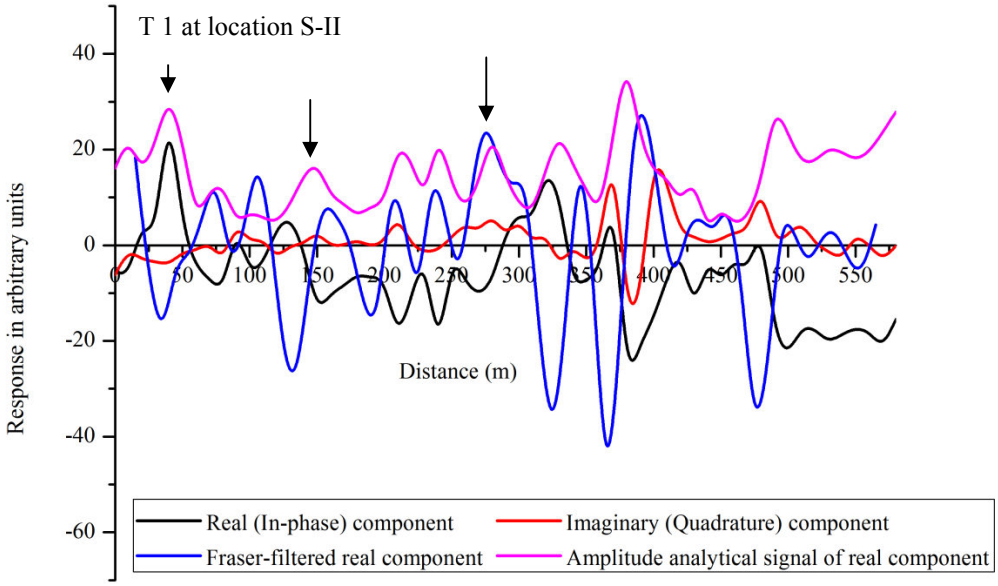
T 1 at location S-II
Response in arbitrary units
Distance (m)
Real (In-phase) component
Imaginary (Quadrature) component
Fraser-filtered real component
Amplitude analytical signal of real component

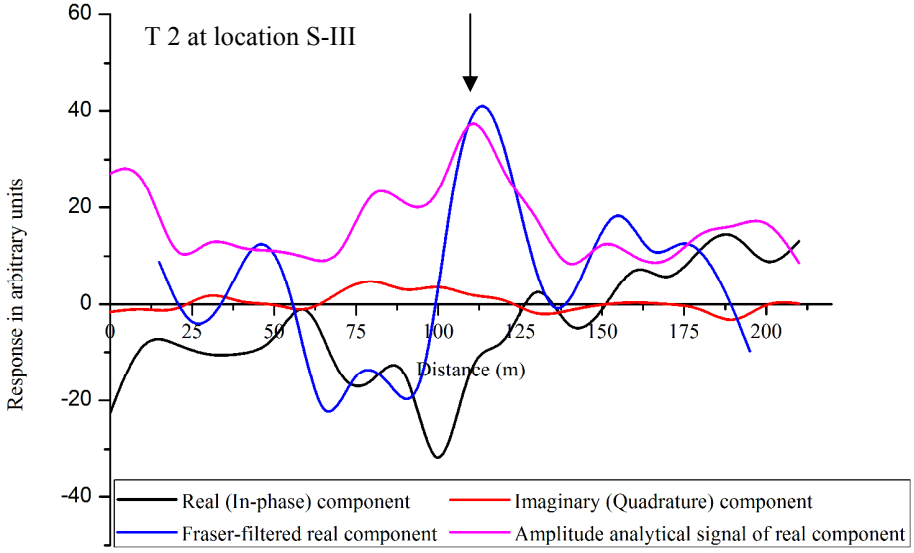
T 2 at location S-III
Response in arbitrary units
Distance (m)
Real (In-phase) component
Imaginary (Quadrature) component
Fraser-filtered real component
Amplitude analytical signal of real component

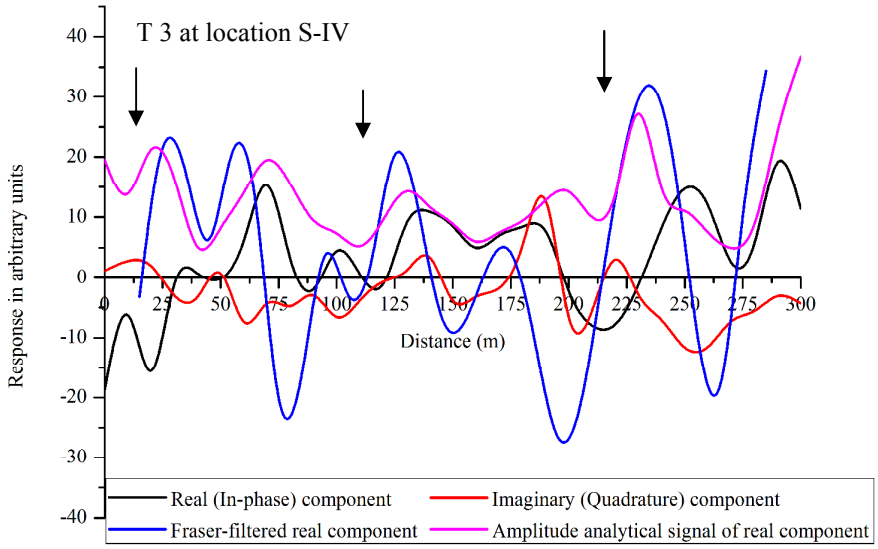
T 3 at location S-IV
Response in arbitrary units
Distance (m)
Real (In-phase) component
Imaginary (Quadrature) component
Fraser-filtered real component
Amplitude analytical signal of real component

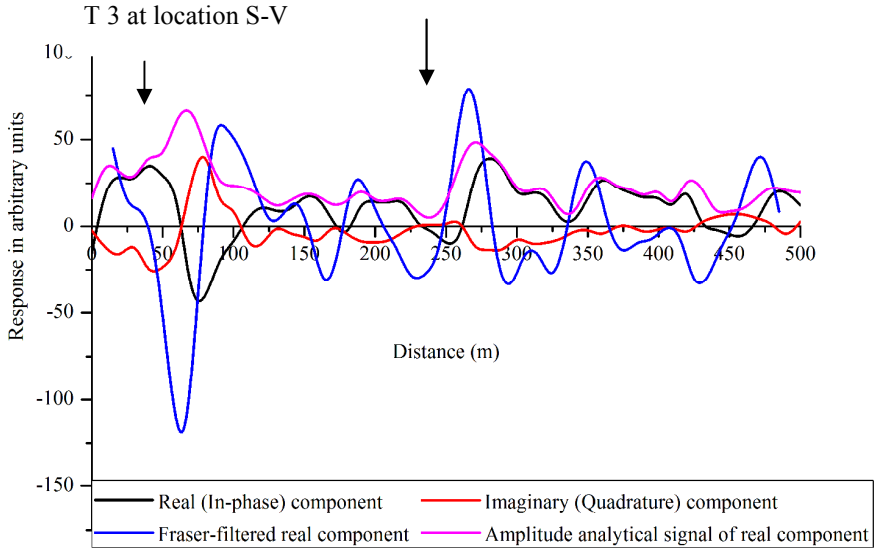
T 3 at location S-V
Response in arbitrary units
Distance (m)
Real (In-phase) component
Imaginary (Quadrature) component
Fraser-filtered real component
Amplitude analytical signal of real component

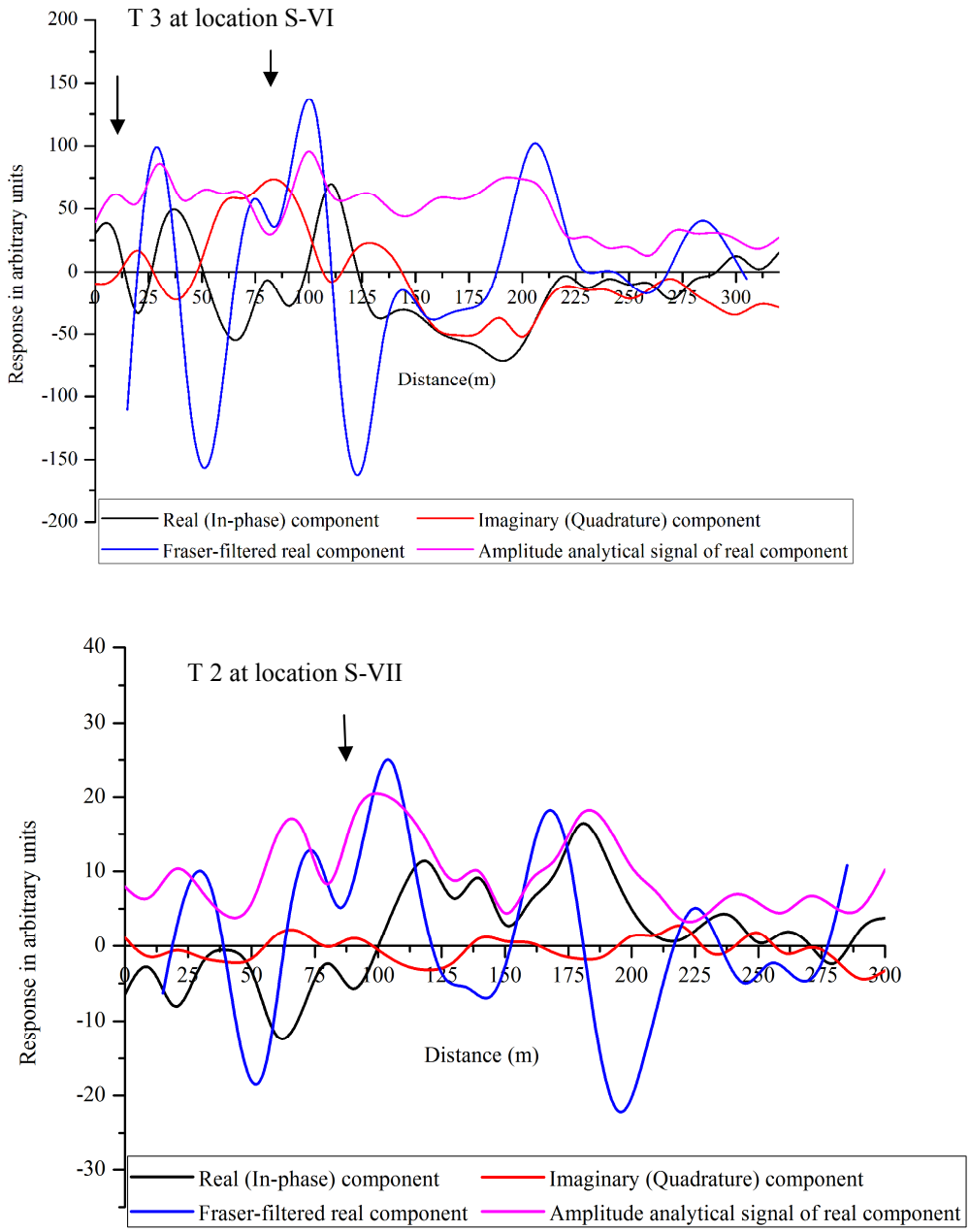

Figure 2 (a). Plot of the in-phase, quadrature, Fraser-filtered and amplitude analytical signal of the in-phase component at different locations of the survey area

Further analysis involved the plotting of the Hilbert transform, amplitude analytical signal and in-phase component of the traverses (Figure 2(b)). Analysis of anomalous body that exists close to where electrical sounding was conducted, were carried out for comparison. Such points are shown in Figure 2(b) with a vertical line and the source marked as x_0. The abscissa of the point of intersection between the in-phase and Hilbert transform over the envisaged anomaly were marked as x_1 and x_2. Based on the procedure of the abscissa of the point of intersection of an anomaly and the Hilbert transform, the approximate depth to the top of the conductors is computed using Equation (7).

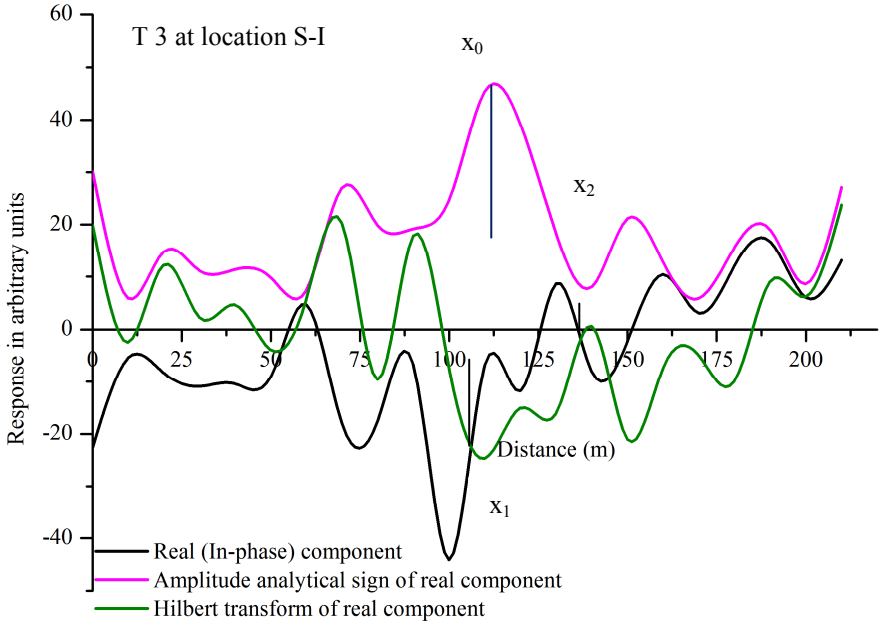
T 3 at location S-I
x0
x2
x1
Response in arbitrary units
Distance (m)
Real (In-phase) component
Amplitude analytical sign of real component
Hilbert transform of real component

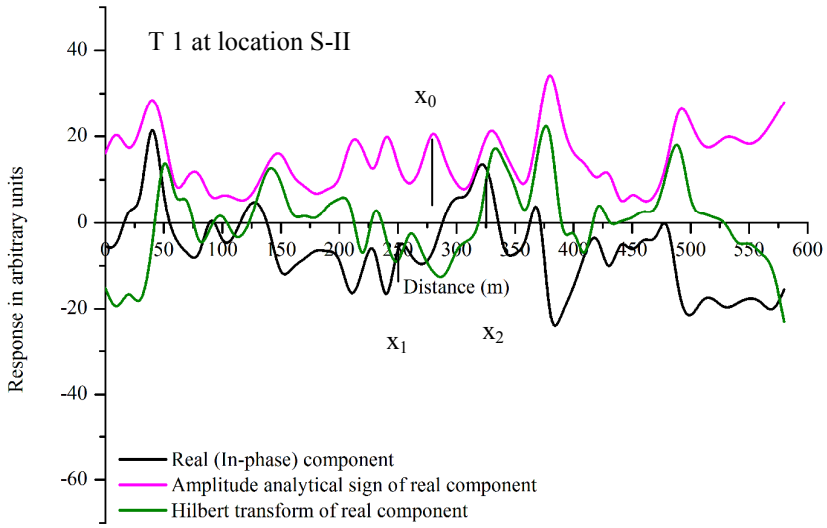
T 1 at location S-II
x0
x1
x2
Response in arbitrary units
Distance (m)
Real (In-phase) component
Amplitude analytical sign of real component
Hilbert transform of real component

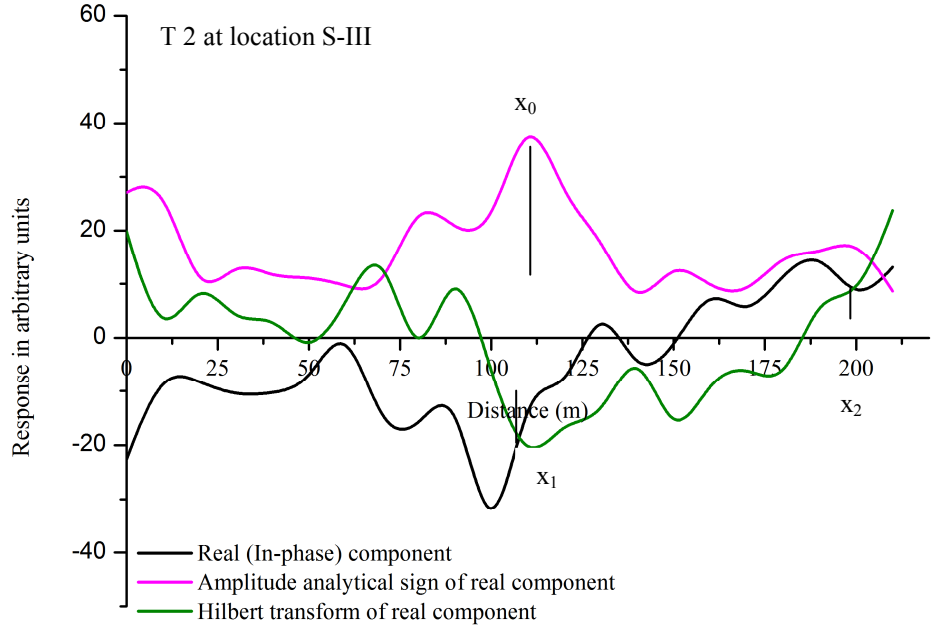
T 2 at location S-III
Response in arbitrary units
Distance (m)
x0
x1
x2
Real (In-phase) component
Amplitude analytical sign of real component
Hilbert transform of real component

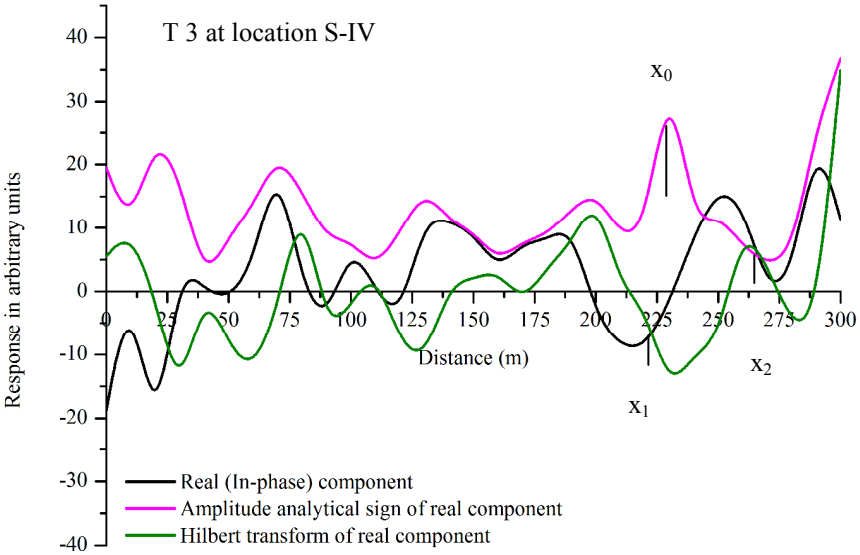
T 3 at location S-IV
Response in arbitrary units
Distance (m)
x0
x1
x2
Real (In-phase) component
Amplitude analytical sign of real component
Hilbert transform of real component

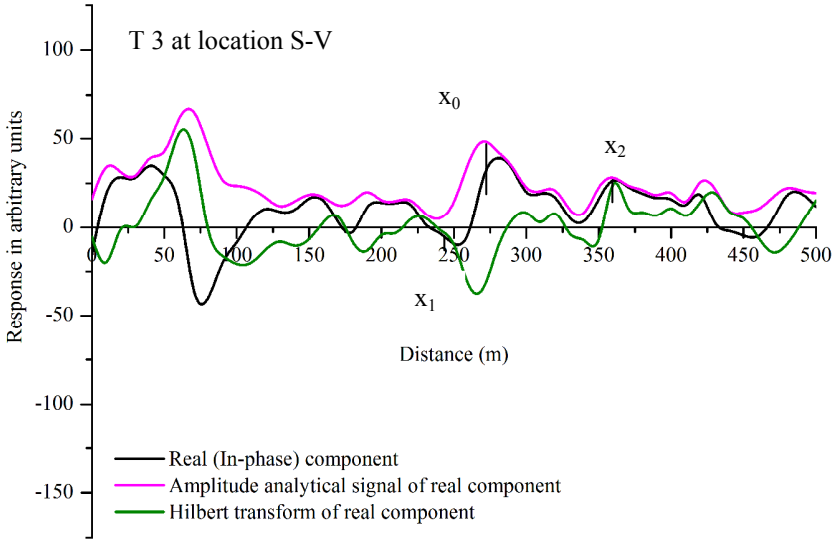
T 3 at location S-V
Response in arbitrary units
Distance (m)
x0
x1
x2
Real (In-phase) component
Amplitude analytical signal of real component
Hilbert transform of real component

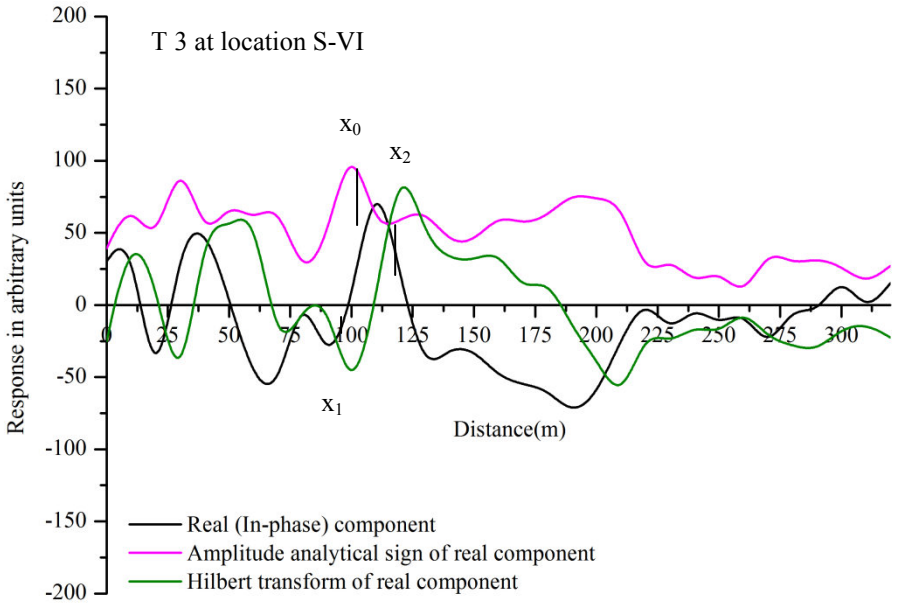
T 3 at location S-VI
Response in arbitrary units
Distance(m)
x0
x1
x2
Real (In-phase) component
Amplitude analytical sign of real component
Hilbert transform of real component

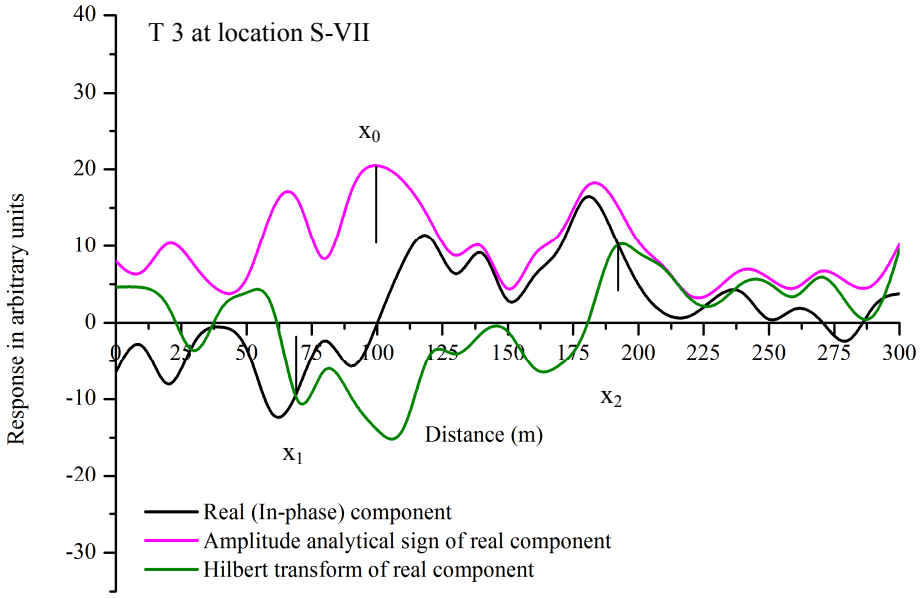

Figure 2 (b). Plot real component of VLF-EM data, its Hilbert transform and amplitude of analytical signal at different locations of the survey area

5.1. Electrical resistivity sounding result

The initial interpretation of the VES data was accomplished using conventional partial curves matching technique utilizing master curves (Koefoed 1979) and the corresponding auxiliary curves (Orellana & Mooney 1966) from which the resistivity values and thicknesses of the layers were obtained. The models derived from the manual interpretation were improved upon through the use of computer iteration technique using the computer algorithm 1X1D (Interprex Ltd 1998) and WinResist Version 1.0 (Vender Velpen 1988) which successfully reduced the interpretation errors to acceptable levels. The computer program has provision of accomplishing three tasks: (i) smoothing of noisy field data, (ii) accurate computation of apparent resistivity models, and (iii) inversion of resistivity data (Vender Velpen 1988). The output is the inverse resistivity model providing layer wise distribution of resistivity value and thickness of the corresponding layer are shown below.

(a)

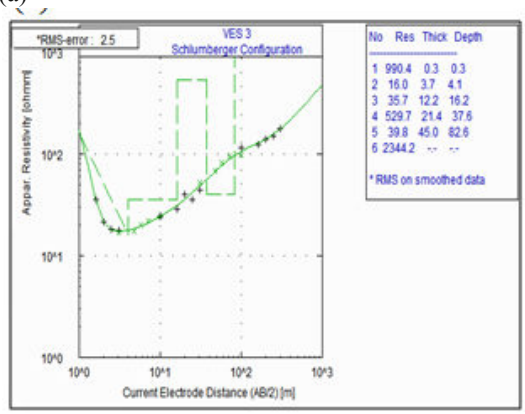

(b)

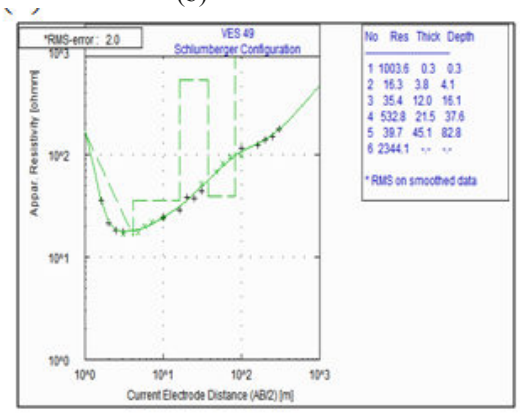

(c)

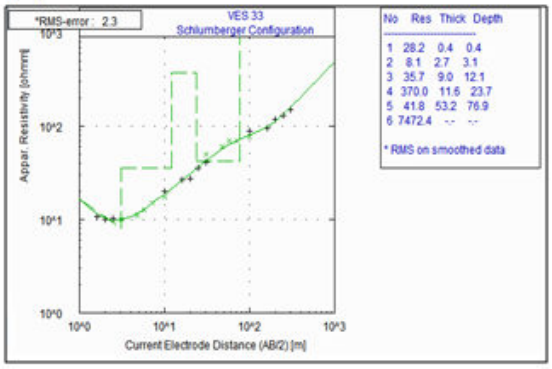

(d)

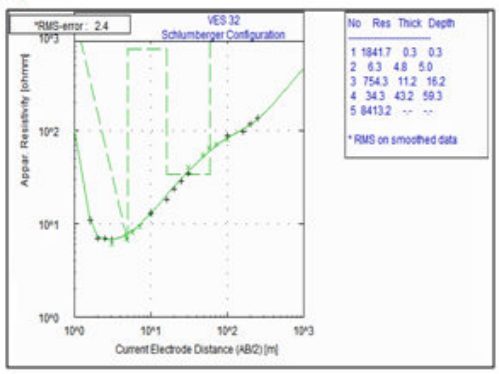

(e)

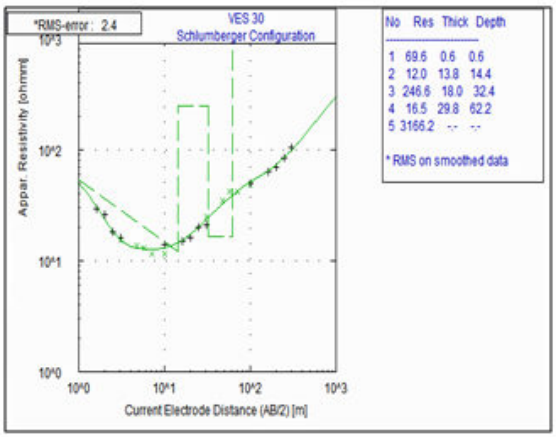

(f)

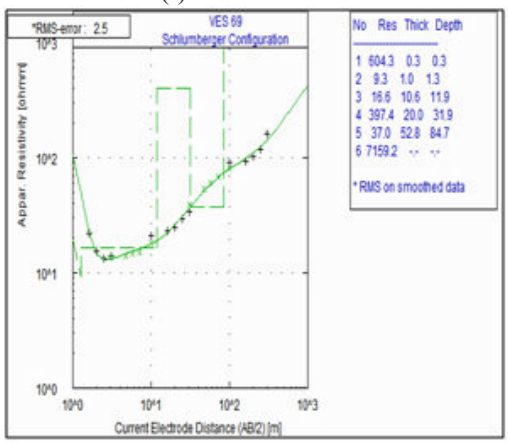

(g)

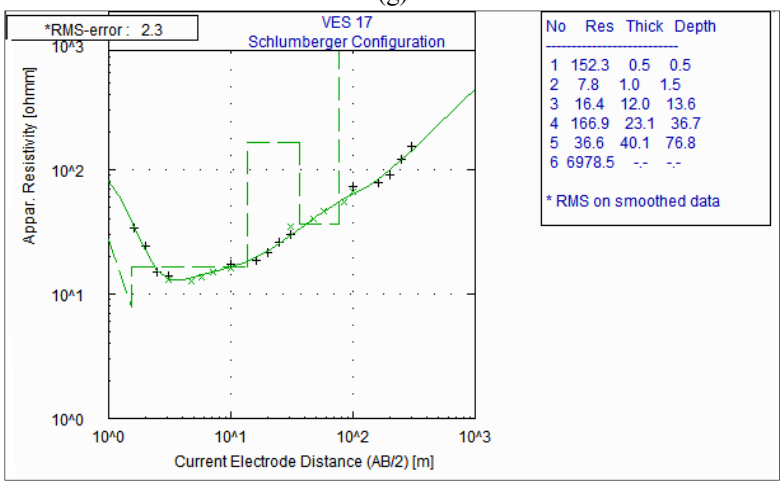

Figure 3 a-g). Model result of VES curves

The computed model of the electrical sounding results depicts four, five and six-layer curves (Figure 3 a-g), and the inferred lithology is presented in Table 1.

Table 1. Geoelectrical and lithologic parameter of the Ves points

VES No.	No. of layers	Apparent resistivity (Ωm)	Thickness (m)	Depth from ground surface (m)	Lithology
3	4	10.3	2.2	0.0	Surface soil
		3.6	4.8	2.2	Clay
		300.1	66.0	7.0	Semi-fractured/weathered sandstone
		3057.9	--	70.8	compacted sandstone
33	6	282	0.4	0.0	Surface soil
		8.1	2.7	0.4	Clay (wet)
		35.2	9.0	3.1	Clay
		37.0	11.6	12.1	Clay/kankar
		41.8	52.3	23.7	Fractured sandstone
		7472.1	--	76.7	Compacted sandstone
49	6	1003.6	0.3	0.0	Surface soil
		16.3	3.8	0.3	Clay
		35.4	12.0	4.1	Clay/kankar
		532.8	21.5	16.1	Semi-fractured/weathered sandstone
		39.7	45.1	37.6	Fractured sandstone
		2344.1	--	82.8	Compacted sandstone
32	5	1841.7	0.3	0.0	Surface soil
		6.3	4.8	0.3	Clay
		754.3	11.2	5.1	Semi-compacted/weathered sandstone
		34.3	43.2	16.3	Fractured sandstone
		8413.2	--	59.4	Compacted sandstone
30	5	696	0.6	0.0	Surface soil
		12.0	13.8	0.6	Clay
		246.6	18.0	14.4	Clay/kankar
		16.5	29.8	32.6	Fractured sandstone
		3166.8	--	62.2	Compacted sandstone
69	6	604.3	0.3	0	Surface soil
		9.3	1.0	0.3	Wet clay
		397.4	20.0	11.9	Semi-compacted/weathered sandstone
		37.0	52.8	31.9	Fractured sandstone
		7159.2	---	84.7	Compacted sandstone
17	6	555	0.5	0.0	Surface soil
		12.3	2.2	0.5	Clay
		34.6	7.8	2.7	Clay/kankar
		410.5	15.7	10.5	Semi-fractured/weathered sandstone
		40.2	40.9	26.2	Fractured sandstone
		10551	--	67.1	Compacted sandstone

A comparison of the result of the depth to the top of the anomaly estimated from the amplitude of the analytical signal analysis and the interpreted vertical electrical sounding id presented in Table 2.

Table 2. Comparison of the depth to the top of a conductor obtained from the analytical signal analysis and the vertical electrical sounding at different locations.

Locations of traverse	Depth from analytical signal analysis (m)	Depth from ves (m)
S-I	8.5	7.0
S-II	21.0	23.7
S-III	42.0	37.6
S-IV	14.0	16.3
S-V	35.0	32.6
S-VI	5.0	31.9
S-VII	30.0	26.2

6. Conclusion

From Table 2, it is observed that the depth to the top of the conductors computed, fairly agrees with the depth obtained from VES survey conducted around the vicinity of the anomaly for all the locations except at location S-VI where the discrepancy is very wide. In addition to the location of the origin of an anomaly, it can be concluded that this analysis procedure is also necessary for the purpose of interpretation of depth.

References

Bhattacharyya, A., (1996), Recent Advances in Vindhyan Geology, *Geol. Soc. India Memoir*, 36, 331.

Bose, P.K., Sarkar, S., Chakrabarty, S. & Banerjee, S. (2001), Overview of Meso- to Neoproterozoic evolution of the Vindhyan basin, *Central India [J]. Sediment. Geol.,* 142, 395–419.

Dondurur, D. & Pamukcu, O.A. (2003), Interpretation of magnetic anomalies from dipping dike model using inverse solution, power spectrum and Hilbert transform, *Journal of Balkan Geophysical Society*, 6(2), 127-136.

Fischer, G., Le Quang, B.V. & Muller, I. (1983), VLF ground surveys, a powerful tool for the study of shallow two-dimensional structures, *Geophys. Prosp*., 31, 977-991.

Interprex Limited (1998), Resix Scientific Software Program. Interprex Limited.

Jeng, Y., Lin, M.J. & Chen, C.S. (2004) A very low frequency-electromagnetic study of the geo-enviromental hazardous areas in Taiwan, *Enviro. Geol.,* 46, 748-795.

Kearey, P. & Brooks, M. (1984), An introduction to geophysical exploration, Blackwell, Oxford, 296.

Koefoed, O. (1979), Geosounding principles, 1: Resistivity Sounding Measurements, Elsevier.

Mohan, N.L, Sundararajan, N. & Seshagiri Rao, S.V. (1982), Interpretation of some two dimensional bodies using the Hilbert transform, *Geophysics*, 47(3), 376–387.

Mohan, N.L., Anand Babu, L. & Seshagiri Rao, S.V. (1986), Gravity interpretation using the Mellin Transform, *Geophysics*, 51(1), 114–122.

Nabighian, M.N. (1972), The analytic signal of two-dimensional magnetic bodies with polygonal cross-section, its properties and use for automated anomaly interpretation, *Geophysics*, 37, 507-512.

Orellana, E. & Mooney, H. M. (1966), Master tables and curves for vertical electrical sounding over layered structures, *Inerciencia*.

Rai, S.N., Thiagarajan, S., Ratna Kumari, Y. Anand Rao, V. & Manglik, A. (2013), Delineation of aquifers in basaltic hard rock terrain using vertical electrical soundings data, *J. Earth Syst. Sci.*, 122(1), 29–41.

Ramesh Babu, V., Ram, S. & Sundararajan, N. (2007), Modeling of magnetic and VLF-EM with an application to basement fractures: a case study from Raigarh, India, *Geophysics,* 71, 133–40.

Sinha, A.K. (1990), Interpretation of ground VLF-EM data interms of inclined sheet-like conductor model, *PAGEOPH*., 132(4), 733-755.

Shendi, E.A. (1997), On the effectiveness of the VLF-method for groundwater prospecting in basement terrains, Sinai Egypt, *Qatar University Science Journal*, 17(1), 143-152.

Srigutomo, W., Harja, A., Sutarno, D. & Kagiyama, T. (2005), Vlf data analysis through transformation into resistivity value: Application to synthetic and field data, *Indonesia Journal of Physics,* 16(4), 127-136.

Sundararajan, N. & Srinivas, Y. (1996), A modified Hilbert transform and its application to self potential interpretation, *J. Appl. Geophys*., 36, 137–43.

Sundararajan, N. & Srinivas, Y. (2010), Fourier-Hilbert versus Hartley_Hilbert transforms with some geophysical applications, *J. Appl. Geophys*., 71, 157-161.

Sundararajan, N. & RamaBrahmam, G. (1997), Spectral analysis of gravity anomalies caused by slab-like structures: a Hartley transform technique, *J. Appl. Geophys.,* 39, 53–61.

Sundararajan, N, Mohan, N.L., Seshagiri Rao, S. V. & Vijaya Raghava, M. S. (1985), Hilbert transform in the interpretation of magnetic anomalies of various components due to a thin infinite dyke, *PAGEOPH.,* 123, 557-566.

Sundararajan, N, Srinivasa Rao, P. & Sunitha, V. (1998), An analytical method to interpret self-potential anomalies caused by 2D inclined sheets, *Geophysics*, 63(5), 1151–1155.
Sundararajan, N., Ramesh Babu, V. & Chaturvedi, A. K. (2011), Detection of basement fractures favourable to Uranium mineralizatio from VLF-EM signal, *J. Geophys. Eng*., 330-340.
Thomas, J. B. (1969), An introduction to statistical communication theory, John-Wiley and Sons, Inc., New York. 639.
Vender Velpen, B.P.A. (1988), A computer processing package for DC resistivity interpretation for IBM compatibles, The Netherlands ITC J. 1–4..